



Thermodynamic modeling of the solidification path of levitated Fe–Co alloys



Justin E. Rodriguez*, Douglas M. Matson

Department of Mechanical Engineering, Tufts University, Medford, MA 02155, USA

ARTICLE INFO

Article history:

Received 21 November 2014

Received in revised form

1 March 2015

Accepted 10 March 2015

Available online 16 March 2015

Keywords:

Iron–Cobalt alloys

Containerless

Metastable

Phase diagram

Thermophysical properties

Partitioning

ABSTRACT

An improved thermodynamic model of the Fe–Co phase diagram has been achieved by incorporating new experimental data that was obtained via containerless processing. Fe–Co samples were prepared with 30, 40, and 50 at% cobalt, and they were processed via electrostatic levitation (ESL). The samples were levitated, melted, and allowed to cool and solidify in a vacuum. If sufficient undercooling was achieved, the metastable phase was observable after the first recalescence, which gives information on the location of the projected metastable phase lines on the phase diagram. Based on these new results, several parameters were adjusted so that the phase lines better represented the experimental metastable data, while the rest of the phase diagram continues to accurately predict previously accepted experimental results. The improved phase diagram allowed for evaluation of key solidification parameters including the partitioning coefficient of the metastable phase, as well as the thermal driving potential for the solidification of the stable phase from the metastable phase.

© 2015 Elsevier Ltd. All rights reserved.

1. Introduction

Containerless processing methods, such as electrostatic levitation (ESL), or electromagnetic levitation (EML), allow a molten sample to undercool below the stable γ -phase (FCC) liquidus temperature over a wide composition range for Iron–Cobalt alloys. If the undercooling is sufficient, the sample can solidify in a 2 step process known as double recalescence, where it first solidifies to the metastable BCC δ -phase before it transforms to the stable FCC γ -phase [1]. Fig. 1 shows a thermal profile of a sample that undercooled and solidified via double recalescence.

The minimum undercooling (ΔT) to achieve double recalescence is equal to the temperature difference between the BCC and FCC liquidus lines, $\Delta T_{\delta\gamma}$ [2]. ΔT_{δ} is the undercooling relative to the metastable phase, and Δt is the delay time. These data points increase the resolution near the FCC–BCC–Liquid peritectic and expand the temperature range over which BCC–Liquid equilibrium can be observed, thus providing insight into improving thermophysical property evaluations which characterize these transformations. In this context, the temperature of the metastable phase can then be superimposed onto the equilibrium phase diagram, as seen in Fig. 2.

The metastable phase diagram can be calculated by suppressing the stable (FCC) phase, and projecting the BCC phase below the

peritectic temperature [3,4]. Previously accepted thermodynamic models for Fe–Co fall short in one of two ways. The first is that the model doesn't accurately represent the metastable phase, which is a result of propagated errors from the stable phase analysis. The second consists of a misrepresented stable phase diagram, which is a result of optimizing either high-temperature Liquid–Solid equilibrium or low-temperature Solid–Solid transformations

The importance of the accuracy of the metastable phase diagram becomes more evident when considering dendrite growth analysis. The growth rate of the metastable phase is a function of its relative undercooling, as well as its partitioning coefficient and liquidus slope [5]. If the transformation thermal driving potential ($\Delta T_{\delta\gamma}$) between BCC and FCC phases is known (as well as several other parameters), then it is possible to calculate the heat flux from the stable phase dendrite as it grows through the metastable phase. That value can then be applied to a given dendrite growth model such that growth velocity can be calculated [2].

There are several previous works that discuss the formation and microstructure of the metastable phase that forms from undercooled Fe–Co melts. Li [6] discussed the microstructure and phase selection in undercooled Fe–Co at% 70 melts using a glass flux technique. Hermann [7] reported on the metastable phase formation in undercooled Fe–Co melts with 30, 40, and 50 at% Co using a ground based EML as well as parabolic flight experiments.

The initial modeling of the iron, cobalt, and iron–cobalt phase diagram was performed by Guillermet [8–10]. Updated pure element parameters for CALPHAD were later published in 1991 by Dinsdale [11] and again in 2001 [12], where the latter supersedes

* Correspondence to: Tufts University, 204 Anderson Hall, 200 College Avenue, Medford, MA 02155, USA.

E-mail address: Justin.Rodriguez@Tufts.edu (J.E. Rodriguez).

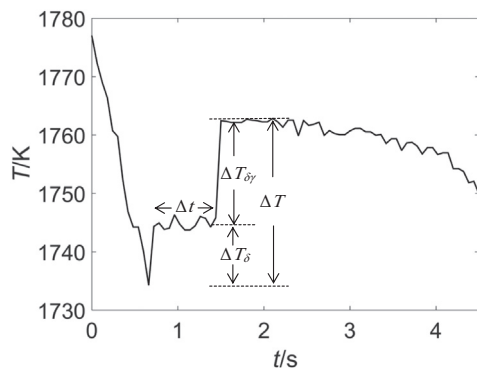


Fig. 1. Thermal profile for Fe–Co at% 40, where the sample is superheated and allowed to undercool and solidify via double recalescence.

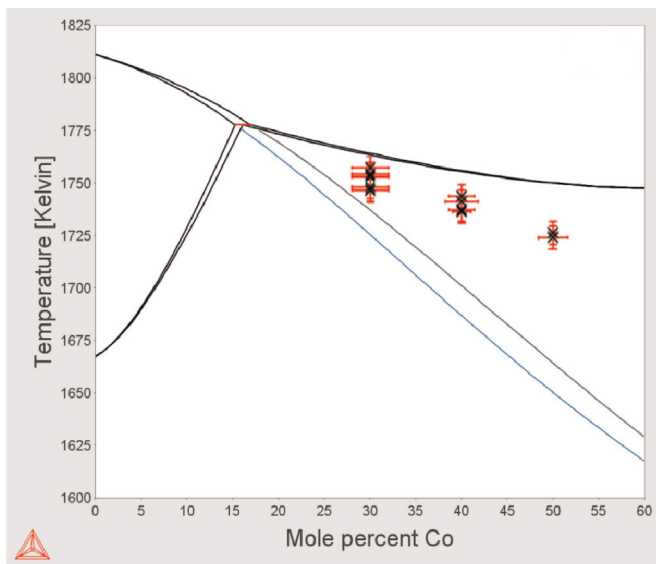


Fig. 2. Equilibrium phase diagram with metastable phase lines calculated in Thermocalc™, using parameters from Guillemet [8–10] and Dinsdale [11,12] with the observed metastable temperatures overlaid: — equilibrium phase lines; — metastable BCC solidus line; — metastable BCC liquidus line; X new observations for the actual metastable transformation temperature from electrostatic levitation test results. Cobalt composition error bars correspond to the evaporation that occurred during the experiment, under the worst case scenario that all of the evaporation was from one component of the system. Temperature error bars correspond to the accuracy of the pyrometer at the given temperature, $\pm 0.3\%$ of reading in $^{\circ}\text{F} + 1.8^{\circ}\text{F}$.

the former. The goal of this work is to improve the accuracy of the phase diagram by incorporating new data from the metastable phase. In doing this, the location of the FCC–BCC–liquid peritectic will be better resolved, there will be a better ability to predict driving potential for solidification in undercooling experiments, and the metastable partitioning coefficient will be obtained. Additionally, the thermophysical properties that are associated with the metastable phase will be more accurately represented, and the solution activity may be determined as a function of constituent such that evaporation during thermal processing may be predicted.

2. Materials and methods

Fe–Co samples were prepared at 30, 40, and 50 at% cobalt, from 99.995% pure iron, and 99.95% pure cobalt, by arc-melting the components under an argon atmosphere, such that they had a mass of approximately 40 mg (~ 2 mm diameter). They were

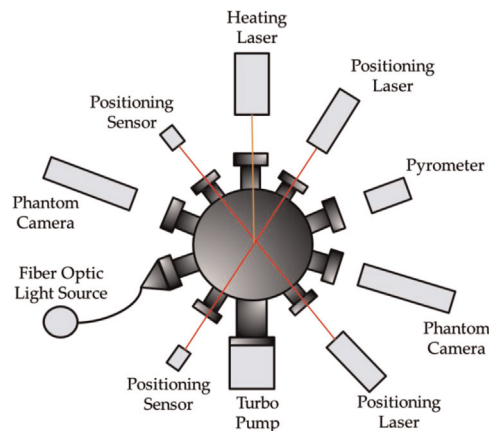


Fig. 3. Top view schematic of the ESL setup at NASA Marshall Space Flight Center.

processed via ESL, where the negatively charged sample was contained within a vacuum chamber (evacuated to $\sim 10^{-5}$ bar), between a negatively charged lower plate, and a positively charged upper plate. A schematic of the ESL setup is given in Fig. 3. The location of the sample was determined by positioning lasers, and the electrostatic field was adjusted accordingly [13]. The sample was then melted, allowed to cool radiatively, and then solidify. The temperature of the samples was monitored with a Mikron Mi-GA140 single color pyrometer, which has a 1.45–1.8 μm wavelength range, and was operating at ~ 16 Hz. The pyrometer accuracy is $\pm 0.3\%$ of reading in $^{\circ}\text{F} + 1.8^{\circ}\text{F}$ for $T < 2732^{\circ}\text{F}$ (1773 K), and $\pm 0.5\%$ of reading in $^{\circ}\text{F}$ for $T > 2732^{\circ}\text{F}$ (1773 K). The pyrometer was calibrated with a Mikron M390 Blackbody generator [14].

The samples were massed prior to arc-melting, after arc-melting, and then again after processing. The total mass evaporation was taken into consideration when the composition error was determined, as represented in Fig. 2.

3. Theory and calculations

3.1. Theory

The fundamental equations that relate free energy to heat capacity, enthalpy, and entropy are given as

$$G = H - TS \quad (1a)$$

$$\partial G / \partial T = -S, \quad (1b)$$

$$\partial^2 G / \partial T^2 = -C_p / T, \quad (1c)$$

where G is the Gibbs free energy, H refers to the enthalpy, S is the entropy, C_p is the constant pressure heat capacity, and T is the temperature. The Fe–Co phase diagram consists of BCC, FCC, HCP, and liquid phases. Therefore, the thermodynamic model must consider each of these phases for both iron and cobalt, as well as the excess free energy and the magnetic contribution. The molar Gibbs energy for the Fe–Co system is given as [10]

$$G_m^{\alpha} = x_1 G_1^{0,\alpha} + x_2 G_2^{0,\alpha} + RT(x_1 \ln(x_1) + x_2 \ln(x_2)) + G_m^{E,\alpha} + \Delta G_m^{mg} \quad (2)$$

The subscripts 1 and 2 correspond to solvent (iron) and solute (cobalt). $G^{0,\alpha}$ represents the molar Gibbs energy of the element, of phase α , where the magnetic contribution is neglected. $G_m^{E,\alpha}$ is the excess free energy of the given phase, and ΔG_m^{mg} is the magnetic contribution. Based on the analysis of previous work, it was

Download English Version:

<https://daneshyari.com/en/article/7955719>

Download Persian Version:

<https://daneshyari.com/article/7955719>

[Daneshyari.com](https://daneshyari.com)